Some additional notes on magnetic reconnection

Magnetic reconnection refers to the topological rearrangement of magnetic-field lines that converts magnetic energy to plasma energy. In these lecture notes, we will assume that such a rearrangement is facilitated by a spatially constant Ohmic resistivity, as might occur in a well-ionized collisional fluid:

$$\frac{\partial \boldsymbol{B}}{\partial t} = \boldsymbol{\nabla} \times (\boldsymbol{u} \times \boldsymbol{B}) + \eta \nabla^2 \boldsymbol{B}.$$

This assumption is obviously not warranted in hot, dilute astrophysical systems, such as the collisionless solar wind, or in poorly ionized systems, like molecular clouds and pre-stellar cores. But let us assume this anyhow, knowing that (i) the physics of reconnection in even the simplest of systems is surprisingly rich and complex, and (ii) there is a huge amount of literature on all aspects of magnetic reconnection in a wide variety of environments. This part of the lecture notes is not intended as a replacement of that literature, nor a synopsis of current research in the field (particularly in the laboratory and the Earth's magnetosheath). What follows is an incomplete presentation of a few key highlights in the theory of magnetic reconnection, which will hopefully provide enough pedagogical value and inspiration to encourage you to dig into the literature further. For that, I recommend that you start with the excellent review articles by Zweibel & Yamada (2009), Yamada *et al.* (2010), and Loureiro & Uzdensky (2016).

.1. Tearing instability

.1.1. *Formulation of the problem*

We begin by analyzing the stability of a simple stationary equilibrium in which the magnetic field reverses across $x = 0$:

$$\boldsymbol{B}_0 = B_y(x)\hat{\boldsymbol{y}} + B_{\rm g}\hat{\boldsymbol{z}}, \tag{.1}$$

where $B_y(x)$ is an odd function and $B_{\rm g} = \text{const}$ denotes the guide field. A oft-employed profile for $B_y(x)$ is the Harris (1962) sheet:

$$B_y(x) = B_{\rm r} \tanh\!\left(\frac{x}{a}\right), \tag{.2}$$

where $B_{\rm r}$ is the asymptotic value of the reconnecting field and a is the characteristic scale length of the current sheet. Its profile, and the associated current density $j_z = (B_{\rm r}/a)\,\mathrm{sech}^2(x/a)$, are shown in the figure below:

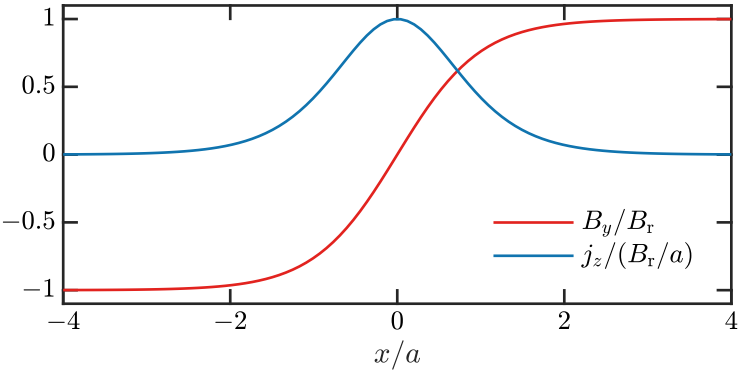

The quickest route through the tearing calculation employs the "reduced MHD" (RMHD) equations governing the evolution of the stream and flux functions Φ and Ψ, respectively, whose gradients describe the (incompressible) velocity and magnetic fields perpendicular to the guide-field axis, $\hat{\boldsymbol{z}}$:[1]

$$\boldsymbol{u}_\perp = \hat{\boldsymbol{z}} \times \boldsymbol{\nabla}_\perp \Phi, \quad \frac{\boldsymbol{B}_\perp}{\sqrt{4\pi\rho}} = \hat{\boldsymbol{z}} \times \boldsymbol{\nabla}_\perp \Psi. \tag{.3}$$

Thus, $B_y(x)/\sqrt{4\pi\rho} = \Psi_0'$ for some equilibrium $\Psi_0(x)$. If $B_y(x)$ is taken to be the Harris-sheet profile (.2), then $\Psi_0 = a v_{\mathrm{A,r}} \ln[\cosh(x/a)]$, where $v_{\mathrm{A,r}} \doteq B_\mathrm{r}/\sqrt{4\pi\rho}$ is the Alfvén speed associated with the reconnecting field. The RMHD equations are

$$\frac{\partial}{\partial t}\Psi + \{\Phi, \Psi\} = v_\mathrm{A} \frac{\partial}{\partial z}\Phi + \eta \nabla_\perp^2 \Psi, \tag{.4}$$

$$\frac{\partial}{\partial t}\nabla_\perp^2 \Phi + \left\{\Phi, \nabla_\perp^2 \Phi\right\} = v_\mathrm{A} \frac{\partial}{\partial z}\nabla_\perp^2 \Psi + \left\{\Psi, \nabla_\perp^2 \Psi\right\} \tag{.5}$$

where the Poisson bracket

$$\{\Phi, \Psi\} \doteq \hat{\boldsymbol{z}} \cdot \left(\boldsymbol{\nabla}_\perp \Phi \times \boldsymbol{\nabla}_\perp \Psi\right). \tag{.6}$$

The first equation (.4) is essentially the induction equation, which includes (from left to right) the time rate of change of the magnetic field, the non-linear advection of the magnetic field by the flow, the linear stretching of the magnetic field by Alfvénic motions, and diffusion by a constant Ohmic diffusivity η. The second equation (.5) is technically an equation for the flow vorticity $\boldsymbol{\omega} = \boldsymbol{\nabla} \times \boldsymbol{u}$, but you can think of it as containing all the same physics as the momentum equation: from left-to-right, the time rate of change of the fluid velocity, the non-linear advection of the velocity by the flow, the linear restoring tension force from the magnetic field on the velocity, and the stress acting on the flow due to the non-linear part of the Lorentz force.

The equilibrium (.1) is perturbed by small fluctuations having no variation along the guide field and a sinusoidal variation along the reconnecting field:

$$\Phi = \phi(x) \mathrm{e}^{\mathrm{i}ky + \gamma t}, \quad \Psi = \Psi_0(x) + \psi(x) \mathrm{e}^{\mathrm{i}ky + \gamma t}, \tag{.7}$$

where k is the wavenumber and γ is the rate at which perturbations will grow or decay. Substituting (.7) into (.5) and (.4) and retaining terms of only linear order in the fluctuation amplitudes, we have

$$\gamma\left(\frac{\mathrm{d}^2}{\mathrm{d}x^2} - k^2\right)\phi = \mathrm{i}k\Psi_0'\left(\frac{\mathrm{d}^2}{\mathrm{d}x^2} - k^2\right)\psi - \mathrm{i}k\psi\Psi_0''', \tag{.8}$$

$$\gamma\psi - \mathrm{i}k\phi\Psi_0' = \eta\left(\frac{\mathrm{d}^2}{\mathrm{d}x^2} - k^2\right)\psi. \tag{.9}$$

The trick to solving this set of equations is to realize that, as η tends towards zero, the

[1] RMHD refers to a reduction of the standard MHD equations that separates Alfvén-wave physics from the physics of compressive (i.e. magnetosonic) fluctuations. It does so formally by stipulating that the characteristic scale along the mean magnetic-field direction of the fluctuations is much larger than the characteristic scale across that direction (among other assumptions either related to the plasma β parameter or to the size of the fluctuations relative to the mean field). But for the purposes of this presentation of tearing mode theory, you can think of these RMHD equations as simply MHD in an incompressible ($\boldsymbol{\nabla} \cdot \boldsymbol{u} = 0$) plasma with the stipulation that Alfvénic physics triumphs. The practical mathematical outcome is that the velocity and magnetic field oriented perpendicularly to the guide magnetic field may be expressed in terms of potential functions.

derivative on the right-hand side of (.9) must grow to balance the terms on the left-hand side. In other words, a boundary layer forms about $x = 0$, outside of which the system satisfies the ideal-MHD equations and inside of which the resistivity is important. The width of this boundary layer is customarily denoted $\delta_{\rm in}$, and much of reconnection theory rests on determining its size given the various attributes of the host plasma. To do so, we will first solve (.8) and (.9) in the "outer region", where the resistivity is negligible and the system behaves as though it were ideal. Then they will be solved in the "inner region", where the resistivity dominates and $k \sim a^{-1} \ll {\rm d}/{\rm d}x \sim \delta_{\rm in}^{-1}$. The two solutions must asymptotically join onto one another; this matching, along with boundary conditions at $x = 0$ and $\pm\infty$, will determine the full solution.

Before proceeding with this program, it will be advantageous to define the resistive and Alfvén timescales,

$$\tau_\eta \doteq \frac{a^2}{\eta} \quad \text{and} \quad \tau_{\rm A} \doteq \frac{1}{ka\Psi_0''(0)} = \frac{1}{kv_{\rm A,r}}, \tag{.10}$$

respectively. We will assume $\tau_\eta^{-1} \ll \gamma \ll \tau_{\rm A}^{-1}$, i.e. the tearing mode grows faster than it takes for the entirety of the current sheet to resistively diffuse but slower than it takes for an Alfvén wave to cross k^{-1}. Physically, this implies that the outer solution results from neglecting the plasma's inertia and Ohmic resistivity.

.1.2. *Outer equation*

Adopting the ordering $\tau_\eta^{-1} \ll \gamma \ll \tau_{\rm A}^{-1}$, equations (.8) and (.9) reduce to

$$\left(\frac{{\rm d}^2}{{\rm d}x^2} - k^2 - \frac{\Psi_0'''}{\Psi_0'}\right)\psi_{\rm out} = 0 \quad \text{and} \quad \phi_{\rm out} = \frac{\gamma}{{\rm i}k\Psi_0'}\psi_{\rm out}. \tag{.11}$$

Note that $\Psi_0'''/\Psi_0' = B_y''/B_y$ measures the gradient of the current density, and so different current-sheet profiles will result in different solutions to (.11). Regardless of the exact current-sheet profile, however, both $\phi_{\rm out}$ and $\psi_{\rm out}$ must tend to zero as $x \to \pm\infty$. Also, since the y-component of the perturbed magnetic field must reverse direction at $x = 0$, $\psi_{\rm out}$ must have a discontinuous derivative there, corresponding to a singular current. Indeed, it is this discontinuity that characterizes the free energy available to reconnect, quantified by the tearing-instability parameter

$$\Delta' \doteq \frac{1}{\psi_{\rm out}(0)}\frac{{\rm d}\psi_{\rm out}}{{\rm d}x}\bigg|_{-0}^{+0}, \tag{.12}$$

and that ultimately warrants consideration of a resistive inner layer.

.1.3. *Inner equation*

In the inner region where $k \ll {\rm d}/{\rm d}x \sim \delta_{\rm in}^{-1}$, the dominant terms in (.8) and (.9) are

$$\gamma\frac{{\rm d}^2\phi_{\rm in}}{{\rm d}x^2} = {\rm i}k\Psi_0'\frac{{\rm d}^2\psi_{\rm in}}{{\rm d}x^2}, \tag{.13}$$

$$\gamma\psi_{\rm in} - {\rm i}k\phi_{\rm in}\Psi_0' = \eta\frac{{\rm d}^2\psi_{\rm in}}{{\rm d}x^2}. \tag{.14}$$

These equations may be solved analytically provided some amenable form of Ψ_0'. Because we are deep within the current sheet, the leading-order term in a Taylor expansion will suffice, *viz.*, $\Psi_0' \approx \Psi_0''(0)x = v_{\rm A,r}(x/a)$. Then (.13) and (.14) may be straightforwardly

combined to obtain

$$\frac{\mathrm{d}^2\psi_{\mathrm{in}}}{\mathrm{d}x^2} = -\left[\frac{\gamma}{k\Psi_0''(0)}\right]^2 \frac{1}{x}\frac{\mathrm{d}^2}{\mathrm{d}x^2}\left[\frac{1}{x}\left(1 - \frac{\eta}{\gamma}\frac{\mathrm{d}^2}{\mathrm{d}x^2}\right)\psi_{\mathrm{in}}\right]. \tag{.15}$$

With some effort, this equation can actually be solved for ψ_{in} analytically. I'll show you how below. But even without that effort, equation (.15) may be used to estimate the width of the boundary layer, δ_{in}:

$$1 \sim (\gamma a \tau_{\mathrm{A}})^2 \frac{\eta}{\gamma \delta_{\mathrm{in}}^4} \quad \Longrightarrow \quad \frac{\delta_{\mathrm{in}}}{a} \sim \left(\frac{\gamma \tau_{\mathrm{A}}^2}{\tau_\eta}\right)^{1/4}. \tag{.16}$$

Note that δ_{in} depends on k – each tearing mode k has a different boundary-layer width; because of this, each k will correspond to a different Δ'.

Normalizing lengthscales to δ_{in} by introducing $\xi \doteq x/\delta_{\mathrm{in}}$, equation (.15) may be written as

$$\frac{\mathrm{d}^2\psi_{\mathrm{in}}}{\mathrm{d}\xi^2} = -\frac{1}{\xi}\frac{\mathrm{d}^2}{\mathrm{d}\xi^2}\left[\frac{1}{\xi}\left(\Lambda - \frac{\mathrm{d}^2}{\mathrm{d}\xi^2}\right)\psi_{\mathrm{in}}\right], \tag{.17}$$

where the eigenvalue $\Lambda \doteq \gamma^{3/2}\tau_{\mathrm{A}}\tau_\eta^{1/2} = \gamma\delta_{\mathrm{in}}^2/\eta$ is the growth rate of the tearing mode normalized by the rate of resistive diffusion across a layer of width δ_{in}. Provided we can solve (.17), the solution ψ_{in} must be matched onto the outer solution ψ_{out}. This is done by equating the discontinuity in ψ_{out}, quantified by Δ' (see (.12)), to the total change in $\mathrm{d}\psi_{\mathrm{in}}/\mathrm{d}x$ across the inner region, *viz.*,

$$\Delta' = \frac{2}{\delta_{\mathrm{in}}}\int_0^1 \mathrm{d}\xi\, \frac{1}{\psi_{\mathrm{in}}(0)}\frac{\mathrm{d}^2\psi_{\mathrm{in}}}{\mathrm{d}\xi^2}.$$

(The factor of 2 is because the solution is odd, and so the total change across the $x = 0$ surface is twice the change measured for $x > 0$.) The upper limit on the integral can be extended to $+\infty$ by committing only a $\sim$10% error:

$$\Delta' = \frac{2}{\delta_{\mathrm{in}}}\int_0^\infty \mathrm{d}\xi\, \frac{1}{\psi_{\mathrm{in}}(0)}\frac{\mathrm{d}^2\psi_{\mathrm{in}}}{\mathrm{d}\xi^2}. \tag{.18}$$

So, find $\psi(\xi)$ by solving the inner equation (.17), compute the integral in (.18), and invert the answer to obtain the growth rate in terms of Δ'.

Before carrying out that program, it will be useful to further simply (.17) by introducing

$$\chi(\xi) \doteq \xi^2 \frac{\mathrm{d}}{\mathrm{d}\xi}\left[\frac{\psi_{\mathrm{in}}(\xi)}{\xi}\right], \tag{.19}$$

so that

$$\frac{\mathrm{d}}{\mathrm{d}\xi}\left[\frac{\mathrm{d}}{\mathrm{d}\xi}\left(\frac{1}{\xi^2}\frac{\mathrm{d}\chi}{\mathrm{d}\xi}\right) - \left(1 + \frac{\Lambda}{\xi^2}\right)\chi\right] = 0. \tag{.20}$$

Integrating this equation once and, for reasons that will eventually become apparent, setting the integration constant to $-\chi_\infty$, we find

$$\xi^2 \frac{\mathrm{d}}{\mathrm{d}\xi}\left(\frac{1}{\xi^2}\frac{\mathrm{d}\chi}{\mathrm{d}\xi}\right) - \left(\xi^2 + \Lambda\right)\chi = -\chi_\infty \xi^2. \tag{.21}$$

Once this equation is solved, the inner solution is obtained using (cf. (.19))

$$\psi_{\mathrm{in}}(\xi) = -\xi\int_\xi^\infty \mathrm{d}x\, \frac{\chi(x)}{x^2} = -\xi\int_\xi^\infty \mathrm{d}x\, \frac{\chi'(x)}{x} - \chi(\xi), \tag{.22}$$

which may then be plugged into (.18) to compute Δ'.

.1.4. *Approximate solutions*

There are a few ways to solve (.11) and (.21), none of which are particularly obvious. However, it's possible to obtain scaling laws for Δ' and the tearing-mode growth rate γ without actually doing so. In fact, the answers obtained in this way differ from those obtained by a more mathematically rigorous solution (see §.1.5) by only order-unity coefficients. Nice.

We start with (.11), the outer equation. With some knowledge that the fastest-growing modes occur at long wavelengths ($ka \ll 1$), we can make some progress by simply dropping the middle term in (.11). Then, so long as B_y varies faster within $|x| \lesssim a$ than it does at $|x| \gg a$, we can estimate

$$\Delta' \sim \frac{1}{ka^2}. \tag{.23}$$

(This scaling is exact for the Harris-sheet profile, solved for in §.1.5.) One may formalize this estimate somewhat (Loureiro *et al.* 2007, 2013) by quantifying what "varies faster within $|x| \lesssim a$ than it does at $|x| \gg a$" means, but not much is gained intuitively by going that route, and the estimate (.23) will suffice.

As for the inner equation (.17), we know from (.21) that, whatever its solution, $\psi_{\rm in}(\xi)$ only depends on the parameter Λ. Thus, equation (.18) may be written as

$$\Delta' \delta_{\rm in} = f(\Lambda) \tag{.24}$$

for some function $f(\Lambda)$. Combining (.23) and (.24) yields an expression for the growth rate, provided we can invert $f(\Lambda)$. Fortunately, we can, at least in certain limits.

The first limit is the so-called "constant-ψ approximation" or "FKR regime", which corresponds to $f(\Lambda) \sim \Lambda \ll 1$ (Furth *et al.* 1963). Then (.24) gives $\Delta' \delta_{\rm in} \sim \Lambda$, so that

$$\boxed{\gamma_{\rm FKR} \sim \tau_{\rm A}^{-2/5} \tau_\eta^{-3/5} (\Delta' a)^{4/5}, \quad \frac{\delta_{\rm in}}{a} \sim \left(\frac{\tau_{\rm A}}{\tau_\eta}\right)^{2/5} (\Delta' a)^{1/5}} \tag{.25}$$

With $\Delta' \sim 1/ka^2$ (see (.23)), these become

$$\frac{\gamma_{\rm FKR}}{v_{\rm A,r}/a} \sim (ka)^{-2/5} S_a^{-3/5}, \quad \frac{\delta_{\rm in}}{a} \sim (ka)^{-3/5} S_a^{-2/5}, \tag{.26}$$

where we have introduced the *Lundquist number*

$$S_a \doteq \frac{a v_{\rm A,r}}{\eta}. \tag{.27}$$

Note that longer wavelengths have faster growth rates (the divergence as $k \to 0$ will be cured in the "Coppi" regime, in which the small-Δ' assumption breaks down – see below). This approximation results from setting $\psi_{\rm in} = \psi_{\rm in}(0)$ on the left-hand side of (.14), so that the inner equation (.14) becomes

$$\gamma \psi_{\rm in}(0) - {\rm i} k \phi_{\rm in} \Psi_0''(0) x = \eta \frac{{\rm d}^2 \psi_{\rm in}}{{\rm d}x^2}, \tag{.28}$$

and so (cf. (.21))

$$\xi^2 \frac{\rm d}{{\rm d}\xi} \left(\frac{1}{\xi^2} \frac{{\rm d}\chi}{{\rm d}\xi} \right) - \xi^2 (\chi - \chi_\infty) = -\Lambda \psi_{\rm in}(0). \tag{.29}$$

In effect, we are assuming that the resistive diffusion time across the inner-layer thickness is much shorter than the instability growth time, i.e., $\gamma \ll \eta/\delta_{\rm in}^2$, so that $\psi_{\rm in}$ can be

approximated as constant on the dynamical time scale. Using (.26) in this inequality requires $S_a \gg (\Delta' a)^4$. This is sometimes called the "small-Δ' regime".

The second limit is the "Coppi regime" or "large-Δ' regime", in which the constant-ψ approximation breaks down and $\gamma \sim \eta/\delta_{\rm in}^2$. This occurs for $\Lambda \sim 1^-$, at which $f(\Lambda) \to \infty$. The growth rate then becomes independent of Δ' and we have

$$\boxed{\gamma_{\rm Coppi} \sim \tau_{\rm A}^{-2/3}\tau_\eta^{-1/3}\,, \quad \frac{\delta_{\rm in}}{a} \sim \left(\frac{\tau_{\rm A}}{\tau_\eta}\right)^{1/3}} \tag{.30}$$

In terms of the tearing-mode wavenumber k and the Lundquist number S_a,

$$\frac{\gamma_{\rm Coppi}}{v_{\rm A,r}/a} \sim (ka)^{2/3} S_a^{-1/3}\,, \quad \frac{\delta_{\rm in}}{a} \sim (ka)^{-1/3} S_a^{-1/3}. \tag{.31}$$

In this limit, the shorter wavelengths have faster growth rates, opposite to the FKR scaling (.26). This suggests a maximally growing mode, whose growth rate $\gamma_{\rm max}$ and wavenumber $k_{\rm max}$ may be estimated by matching the FKR solution (.26) to the Coppi one (.31):

$$\gamma_{\rm FKR} \sim \gamma_{\rm Coppi} \quad \Longrightarrow \quad k_{\rm max} a \sim S_a^{-1/4}\,, \quad \frac{\gamma_{\rm max}}{v_{\rm A,r}/a} \sim S_a^{-1/2}\,, \quad \frac{\delta_{\rm in}}{a} \sim S_a^{-1/4}. \tag{.32}$$

Note that the FKR (Coppi) regime corresponds to $k > k_{\rm max}$ ($k < k_{\rm max}$).

Of course, all of these scalings make sense only if the modes can fit into the current sheet, i.e., $kL \gtrsim 1$, where L is the length of the current sheet. For the maximally growing mode to be viable thus requires a current-sheet aspect ratio of $L/a \gtrsim S_a^{1/4}$. If this inequality is not satisfied, then the fastest-growing mode will be the FKR mode (.26) with the smallest possible allowed wavenumber, $kL \sim 1$. Thus, low-aspect-ratio sheets with $L/a \ll S_a^{1/4}$ will develop tearing perturbations comprising just one or two islands; the high-aspect-ratio sheets, in which the Coppi regime is accessible, will instead spawn whole chains comprising $\sim k_{\rm max} L$ islands.

.1.5. *Exact solution for a Harris sheet*

This is **optional** material detailing a more rigorous derivation of the tearing-mode dispersion relation.

The solutions obtained in the last section should suffice for this course. But with some (read: a lot of) effort, one can be more precise. For that task, let us adopt the equilibrium flux function $\Psi_0 = a v_{\rm A,r} \ln[\cosh(x/a)]$, corresponding to the Harris-sheet profile (.2). Then (.11) becomes

$$\left[\frac{{\rm d}^2}{{\rm d}x^2} - k^2 + \frac{2}{a^2}\,{\rm sech}^2\!\left(\frac{x}{a}\right)\right]\psi_{\rm out} = 0 \quad \text{and} \quad \phi_{\rm out} = -{\rm i}\gamma\tau_{\rm A}\coth\!\left(\frac{x}{a}\right)\psi_{\rm out}. \tag{.33}$$

The former equation can be solved by changing variables to $\mu = \tanh(x/a)$, so that ${\rm sech}^2(x/a) = (1-\mu^2)^{-1}$ and

$$\frac{\rm d}{{\rm d}x} = \frac{1-\mu^2}{a}\frac{\rm d}{{\rm d}\mu}, \quad \frac{{\rm d}^2}{{\rm d}x^2} = \frac{1-\mu^2}{a}\frac{\rm d}{{\rm d}\mu}\frac{1-\mu^2}{a}\frac{\rm d}{{\rm d}\mu}.$$

Then (.33) becomes

$$\left[\frac{\rm d}{{\rm d}\mu}(1-\mu^2)\frac{\rm d}{{\rm d}\mu} + 2 - \frac{k^2a^2}{1-\mu^2}\right]\psi_{\rm out} = 0 \quad \text{and} \quad \phi_{\rm out} = -{\rm i}\gamma\tau_{\rm A}\frac{\psi_{\rm out}}{\mu}, \tag{.34}$$

the first of which you might recognize as the associated Legendre equation

$$\left[\frac{\mathrm{d}}{\mathrm{d}\mu}(1-\mu^2)\frac{\mathrm{d}}{\mathrm{d}\mu}+\ell(\ell+1)-\frac{m^2}{1-\mu^2}\right]P_\ell^m(\mu)=0$$

with $\ell=1$ and $m=ka$. Transforming the boundary conditions $\psi(\pm\infty)=0$ into $\psi(\mu=\pm1)=0$ and enforcing $\psi(\mu)=\psi(-\mu)$, the solution to (.34) is thus

$$\psi_{\rm out}=C_{1m}P_1^m(\mu), \tag{.35}$$

with $C_{1m}=$ const. If you can't picture in your head what the first associated Legendre polynomial with non-integer m looks like – I know I can't – you may like to know that the outer solution may be equivalently written as

$$\psi_{\rm out}(x)=C'_{1m}\mathrm{e}^{-kx}\left[1+\frac{1}{ka}\tanh\left(\frac{x}{a}\right)\right] \tag{.36}$$

for $\xi\geqslant0$, where $C'_{1m}=$ const. (Note that $\psi_{\rm out}(-\xi)=\psi_{\rm out}(\xi)$.) Visually:

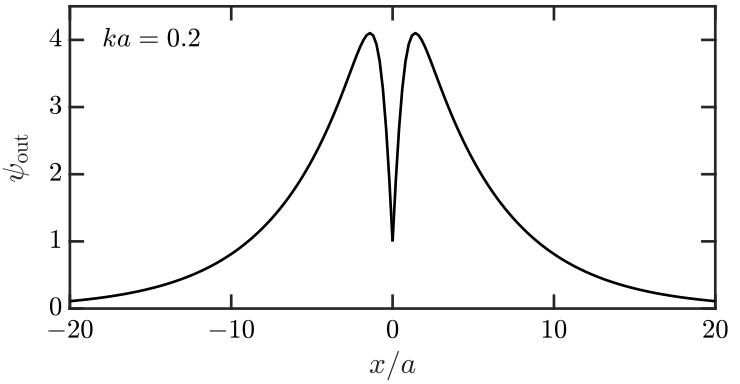

Recall that Δ' measures the discontinuity of $\mathrm{d}\psi_{\rm out}/\mathrm{d}x$ at $x=0$ (see (.12)). Solving for C_{1m} (or C'_{1m}) requires matching onto the inner solution, but even before doing that we can compute Δ' using $\psi_{\rm out}\propto P_1^m(\mu)$ in (.12):[2]

$$\begin{aligned}\Delta' a&=\frac{1}{P_1^m(0)}\frac{\mathrm{d}P_1^m}{\mathrm{d}\mu}\bigg|_{-0}^{+0}=\frac{2}{P_1^m(0)}\frac{\mathrm{d}P_1^m}{\mathrm{d}\mu}\bigg|_{\mu=0}=2\left(\frac{1}{m}-m\right)\\&=2\left(\frac{1}{ka}-ka\right).\end{aligned} \tag{.37}$$

Note that $\Delta'>0$ requires $ka<1$ – any unstable mode must have an extent at least as large as the current-sheet thickness. This places an upper limit on the wavenumber of the FKR modes (.26).

As for the inner equation, let us use its compact form (.21), repeated here for convenience:

$$\xi^2\frac{\mathrm{d}}{\mathrm{d}\xi}\left(\frac{1}{\xi^2}\frac{\mathrm{d}\chi}{\mathrm{d}\xi}\right)-\left(\xi^2+\Lambda\right)\chi=-\chi_\infty\xi^2, \tag{.38}$$

where $\Lambda\doteq\gamma^{3/2}\tau_{\rm A}\tau_\eta^{1/2}$. There are a few ways to solve (.38), none of which are particularly

[2]See https://dlmf.nist.gov/14.5 for information on $P_\ell^m(0)$ and $\mathrm{d}P_\ell^m/\mathrm{d}\mu|_{\mu=0}$.

obvious. One way, explained in Appendix A of Ara *et al.* (1978), is as follows. Write

$$\chi = \chi_\infty \sum_{n=0}^{\infty} a_n L_n^{(-3/2)}(\xi^2)\, \mathrm{e}^{-\xi^2/2}, \tag{.39}$$

where $L_n^\alpha(z)$ are the associated Laguerre (or "Sonine") polynomials satisfying

$$z\frac{\mathrm{d}^2 L_n^{(\alpha)}}{\mathrm{d}z^2} + (\alpha+1-z)\frac{\mathrm{d}L_n^{(\alpha)}}{\mathrm{d}z} + nL_n^{(\alpha)} = 0. \tag{.40}$$

Substitute this decomposition into (.21) and use the recursion relations

$$\frac{\mathrm{d}L_n^\alpha}{\mathrm{d}z} = -L_{n-1}^{\alpha+1}(z) \text{ if } 1 \leqslant n \ (= 0 \text{ otherwise}),$$
$$nL_n^{(-3/2)}(z) = -\left(z+\frac{1}{2}\right)L_{n-1}^{(-1/2)}(z) - zL_{n-2}^{(1/2)}(z),$$

to obtain

$$\sum_{n=0}^{\infty} a_n\, \xi^{-2}\, \mathrm{e}^{-\xi^2/2} L_n^{(-3/2)}(\xi^2)\big(4n+\Lambda-1\big) = 1. \tag{.41}$$

Multiply this by $\mathrm{e}^{-\xi^2/2}\xi^{-1}L_m^{-3/2}$, integrate, and use the orthogonality relation

$$\int_0^\infty \mathrm{d}z\, \mathrm{e}^{-z} z^\alpha L_m^\alpha L_n^\alpha = \delta_{mn}\frac{\Gamma(n+\alpha+1)}{\Gamma(n+1)}$$

to find that

$$\begin{aligned} a_n \frac{(n-3/2)!}{n!}(4n+\Lambda-1) &= \int_0^\infty \mathrm{d}z\, z^{-1/2}\mathrm{e}^{-z/2} L_n^{-3/2} \\ &= \int_0^\infty \mathrm{d}z\, z^{-1/2}\mathrm{e}^{-z/2}(L_n^{-1/2} - L_{n-1}^{-1/2}) \\ &= \sqrt{2}(-1)^n\left[\frac{\Gamma(n+1/2)}{\Gamma(n+1)} + \frac{\Gamma(n-1/2)}{\Gamma(n)}\right] \\ \implies \quad a_n &= \frac{(-1)^n}{\sqrt{2}}\frac{4n-1}{4n+\Lambda-1}. \end{aligned}$$

Thus, equation (.39) becomes[3]

$$\chi = \frac{\chi_\infty}{\sqrt{2}}\,\mathrm{e}^{-\xi^2/2}\sum_{n=0}^{\infty}(-1)^n L_n^{-3/2}(\xi^2)\frac{4n-1}{4n+\Lambda-1} = \xi^2\frac{\mathrm{d}}{\mathrm{d}\xi}\frac{\psi_{\mathrm{in}}}{\xi}, \tag{.42}$$

which may be solved for ψ_{in} following (.22).

Actually doing so and plugging the solution into (.18) to compute Δ' ain't easy, as it involves a lot of non-standard math. I may LaTeX those steps up one day, but, for now, I'll just skip to the answer:

$$\Delta'\delta_{\mathrm{in}} = f(\Lambda) \doteq \frac{\pi}{2}\frac{\Gamma[(\Lambda+3)/4]}{\Gamma[(\Lambda+5)/4]}\frac{\Lambda}{1-\Lambda}. \tag{.43}$$

This is an implicit equation for Γ, which may be solved numerically (see figure below). But it's possible to recover our approximate results (.25) and (.30) in their respective

[3]Note that we cannot use the expansion (.39) if $\Lambda = 1$.

limits. For $\Lambda \ll 1$,

$$f(\Lambda) \approx \frac{\pi}{2}\frac{\Gamma(3/4)}{\Gamma(5/4)}\Lambda \simeq 2.124\,\Lambda \quad \Longrightarrow \quad \gamma \approx 0.547\,\tau_{\rm A}^{-2/5}\tau_\eta^{-3/5}(\Delta' a)^{4/5}. \tag{.44}$$

Our approximate result for this FKR regime, equation (.25), is off by only a factor of 0.547 – not too bad. For $\Lambda = 1^-$,

$$f(\Lambda) \approx \frac{\pi}{2}\frac{\Gamma(1)}{\Gamma(3/2)}\frac{1}{1-\Lambda} = \frac{\sqrt{\pi}}{1-\Lambda} \quad \Longrightarrow \quad \gamma \approx \tau_{\rm A}^{-2/3}\tau_\eta^{-1/3} - \mathcal{O}\left(\frac{k v_{\rm A,r}}{\Delta' a}\right). \tag{.45}$$

This matches our Coppi-regime estimate, (.30). These asymptotic solutions actually do rather well across the full range of wavenumbers:

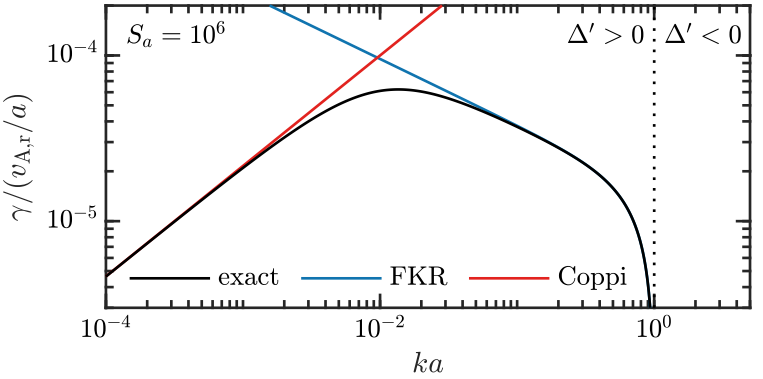

It also appears that we are well justified in estimating the maximally growing mode by matching the FKR and Coppi expressions (as in (.32)). These regimes also occur where we anticipated, with $f(\Lambda) = \Delta'\delta_{\rm in}$ being $\ll 1$ ($\gg 1$) in the FKR (Coppi) regime:

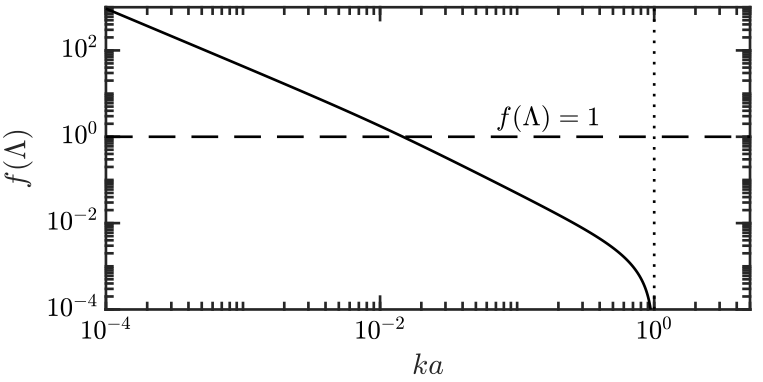

Thus the "small-Δ'" / "large-Δ'" phraseology.

.1.6. *Nonlinear evolution and X-point collapse*

How long does this linear phase, in which the tearing modes grow exponentially, last? That depends on the Δ' of the mode. If the Coppi regime is accessible – i.e., if the maximally growing wavenumber $k_{\rm max}$ (see (.32)) that results in $\Delta'\delta_{\rm in} \gtrsim 1$ also satisfies $k_{\rm max}a < 1$ – then X-point collapse is essentially instantaneous once the width $w = 4\sqrt{-\psi(0)/\Psi_0''(0)}$ of the exponentially growing island reaches $\delta_{\rm in}$. At this moment, $w\Delta'$ is also $\sim$1, and so the deformations of the current sheet by the nonlinear islands have driven the regions between the X-points to marginal stability. If the fastest-growing available

modes are instead FKR-like, then there is a gap between when the nonlinear regime begins ($w \sim \delta_{\rm in}$) and when it ends ($w\Delta' \sim 1$). In between occurs a period of secular growth called the Rutherford (1973) stage, in which $\dot{w} \sim \eta\Delta'(w)$, the argument of Δ' indicating that the logarithmic derivative of $\psi_{\rm out}$ is to be taken across the island (rather than across the inner-layer width).[4] During this slow growth stage, the initially unstable current profile flattens and conditions are set up for the collapse of the inter-island X points (Waelbroeck 1993; Loureiro *et al.* 2005). The figure below, adapted from Loureiro *et al.* (2005), shows contours of ψ at the beginning of X-point collapse (left) and the formation of an embedded, high-aspect ratio current sheet (right):

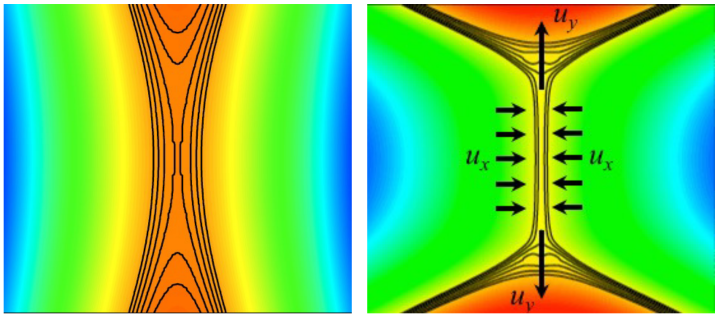

This current sheet is reminiscent of the now-famous Sweet–Parker configuration.

.2. Sweet–Parker reconnection

Peter Sweet (Sweet 1958) and Eugene Parker (Parker 1957) provided the first quantitative model of magnetic reconnection, envisioning it to be a steady-state process in which a two-dimensional, incompressible flow advects magnetic flux into a current sheet of length L and thickness $\delta_{\rm SP} \ll L$. It is through the latter dimension that plasma, accelerated in the direction along the current sheet by magnetic tension, is expelled in the form of an outflow:

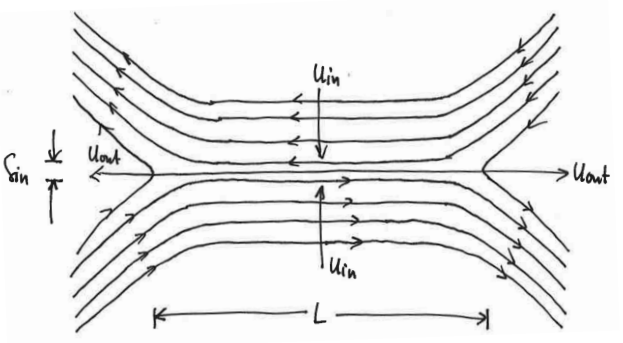

Steady state is achieved by (i) balancing the inflow velocity $u_{\rm in}$ and the outflow velocity $u_{\rm out}$ using mass conservation, $u_{\rm in}L \sim u_{\rm out}\delta_{\rm SP}$; (ii) balancing the advective and resistive electric fields so that all the inflowing magnetic flux is resistively destroyed, $u_{\rm in}v_{\rm A,r} \sim \eta j_z \sim \eta v_{\rm A,r}/\delta_{\rm SP}$; and (iii) stipulating that the outflows are Alfvénic, $u_{\rm out} \sim v_{\rm A,r}$. (This

[4] Rutherford (1973) did not predict a saturation amplitude for the algebraically growing nonlinear tearing mode. Subsequent papers by Militello & Porcelli (2004) and Escande & Ottaviani (2004) ("POEM") derived a modified equation for the Rutherford stage, $\dot{w} \sim \eta(\Delta' - \alpha w/a^2)$ with α being a constant dependent upon the initial current-sheet geometry, thus predicting a saturated amplitude $w \sim \Delta' a^2$.

final ingredient follows from conservation of energy, with the magnetic energy flux into the sheet balancing the kinetic energy flux out of the sheet.) The result is

$$\frac{u_{\rm in}}{v_{\rm A,r}} \sim \frac{\delta_{\rm SP}}{L} \sim \left(\frac{v_{\rm A,r}L}{\eta}\right)^{-1/2} \doteq S^{-1/2}, \tag{.46}$$

where S is the Lundquist number (using the current-sheet length L as the normalizing lengthscale). In the solar corona, $S \sim 10^{12}$–10^{14}; in the Earth's magnetotail, $S \sim 10^{15}$–10^{16}; and in a modern tokamak like JET, $S \sim 10^{6}$–10^{8}. You can see that $S^{-1/2}$ is typically a very small number, and so Sweet–Parker (SP) reconnection is *slow* – not as slow as pure resistive diffusion, but slow in the sense that the reconnection rate $\tau_{\rm r}^{-1} \doteq u_{\rm in}/L \sim (v_{\rm A,r}/L)\, S^{-1/2}$ tends towards zero as $S \to \infty$. For example, the SP model predicts that a reconnection-driven solar flare in a $S \sim 10^{14}$ part of the solar corona should last ∼2 mths; instead, flares are observed to last between 15 min and 1 hr. Not good.

This mismatch between theory and observation was immediately appreciated, and spawned several attempts to formulate a model in which fast reconnection occurs. The culprit is the smallness of the resistive layer: the fact that it must be thin enough to make the current density large also means that the outflowing mass must pass through too small of an opening. One particularly notorious attempt to circumvent this constraint was proposed by Petschek (1964) (later revisited and amended by Kulsrud (2001)), in which the current-sheet length L was shortened at the expense of introducing four standing slow-mode shocks emanating from a central diffusion region:

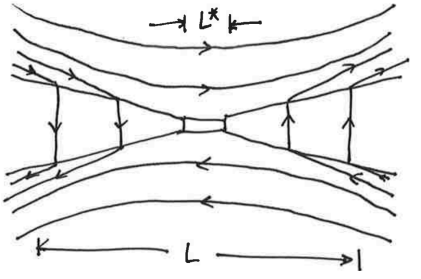

The result is a logarithmic dependence of the reconnection rate on S, $\tau_{\rm r}^{-1} \sim (v_{\rm A,r}/L) \ln S$. Unfortunately, no convincing evidence for this type of reconnection has been found (Park *et al.* 1984; Biskamp 1986; Uzdensky & Kulsrud 2000; Malyshkin *et al.* 2005; Loureiro *et al.* 2005), even when Petschek's solution is used as an initial condition (Uzdensky & Kulsrud 2000).[5]

It is worth emphasizing that the failure of the SP model to explain magnetic reconnection as it occurs in nature is not due to any shortcoming of the theory itself. There are no obvious mistakes in the theory, which has been put on a rigorous footing (e.g., Uzdensky & Kulsrud 2000). Indeed, both numerical simulations (e.g., see figure 4(*b*) of Loureiro *et al.* 2005) and laboratory experiments (e.g., Ji *et al.* 1998) have measured reconnection rates in excellent agreement with the SP scalings (.46). What, then, is the issue?

.3. Plasmoid instability

Let us suspend judgement for the meantime and suppose that the SP model is correct. With tearing-mode theory in hand, let us ask the intriguing question of whether or not

[5]Petschek-like configurations do emerge when strongly localized (anomalous) resistivity profiles are used (Malyshkin *et al.* 2005; Sato & Hayashi 1979; Ugai 1995; Scholer 1989; Erkaev *et al.* 2000, 2001; Biskamp & Schwarz 2001), as might occur under collisionless conditions.

the steady-state SP current sheet is stable to tearing instabilities. One could of course go the route of rigorously doing the linear tearing theory using the SP solution as the background state, as Loureiro *et al.* (2007) did in a now-classic paper, but for our purposes it will be sufficient to simply replace the current-sheet thickness a in the tearing-mode theory of §.1 with $\delta_{\rm SP} \sim S^{-1/2}L$ (Tajima & Shibata 1997; Bhattacharjee *et al.* 2009; Loureiro *et al.* 2013). Focusing on the maximally growing tearing mode (.32),

$$k_{\rm max}L \sim \frac{L}{a}S_a^{-1/4} \longrightarrow \frac{L}{\delta_{\rm SP}}\left(\frac{v_{\rm A,r}\delta_{\rm SP}}{\eta}\right)^{-1/4} \sim S^{3/8}, \tag{.47a}$$

$$\frac{\gamma_{\rm max}}{v_{\rm A,r}/L} \sim \frac{L}{a}S_a^{-1/2} \longrightarrow \frac{L}{\delta_{\rm SP}}\left(\frac{v_{\rm A,r}\delta_{\rm SP}}{\eta}\right)^{-1/2} \sim S^{1/4}, \tag{.47b}$$

$$\frac{\delta_{\rm in}}{L} \sim \frac{a}{L}S_a^{-1/4} \longrightarrow \frac{\delta_{\rm SP}}{L}\left(\frac{v_{\rm A,r}\delta_{\rm SP}}{\eta}\right)^{-1/4} \sim S^{-5/8}. \tag{.47c}$$

This is the *plasmoid instability* – essentially, the tearing instability of a SP current layer. Of course, the situation in question is very different than that obtained using the stationary equilibrium Harris sheet, perhaps most obviously because the former has background flows. These flows can be stabilizing in the tearing calculation, a possibility we have ignored in making the estimates in (.47). This may be circumvented, however, by demanding that $\gamma \gg v_{\rm A,r}/L$, $k_{\rm max}L \gg 1$, and $\delta_{\rm in}/\delta_{\rm SP} \ll 1$ – demands that may be satisfied if $S \gtrsim 10^4$. Indeed, it is at this critical Lundquist number that the plasmoid instability is (now routinely) observed to occur in numerical simulations of reconnection (e.g., Samtaney *et al.* 2009; Daughton *et al.* 2009; Bhattacharjee *et al.* 2009; Ni *et al.* 2010; Huang & Bhattacharjee 2010; Loureiro *et al.* 2012, 2013). The example below is taken from a resistive-MHD numerical simulation by Samtaney *et al.* (2009), showing the evolution of the current density (color) in the central $x = [-\delta_{\rm SP}, \delta_{\rm SP}]$ region of a SP current sheet with $S = 10^7$:

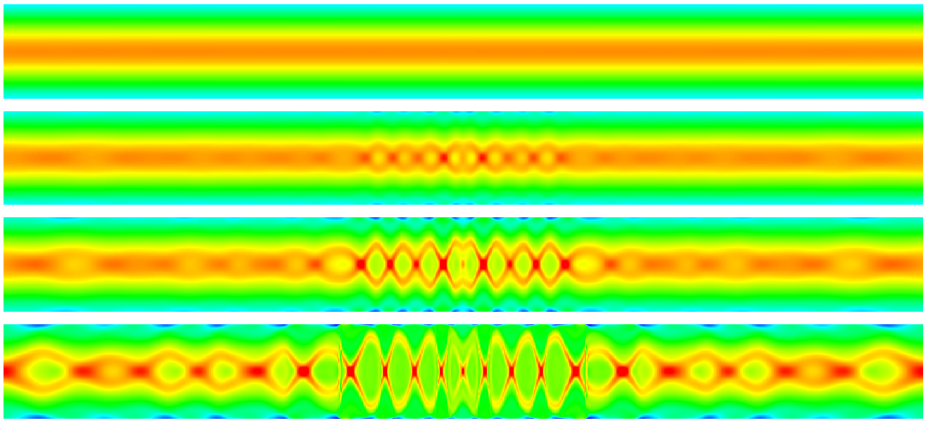

Below is another example, taken from Bhattacharjee *et al.* (2009) using $S = 2\pi \times 10^5$:

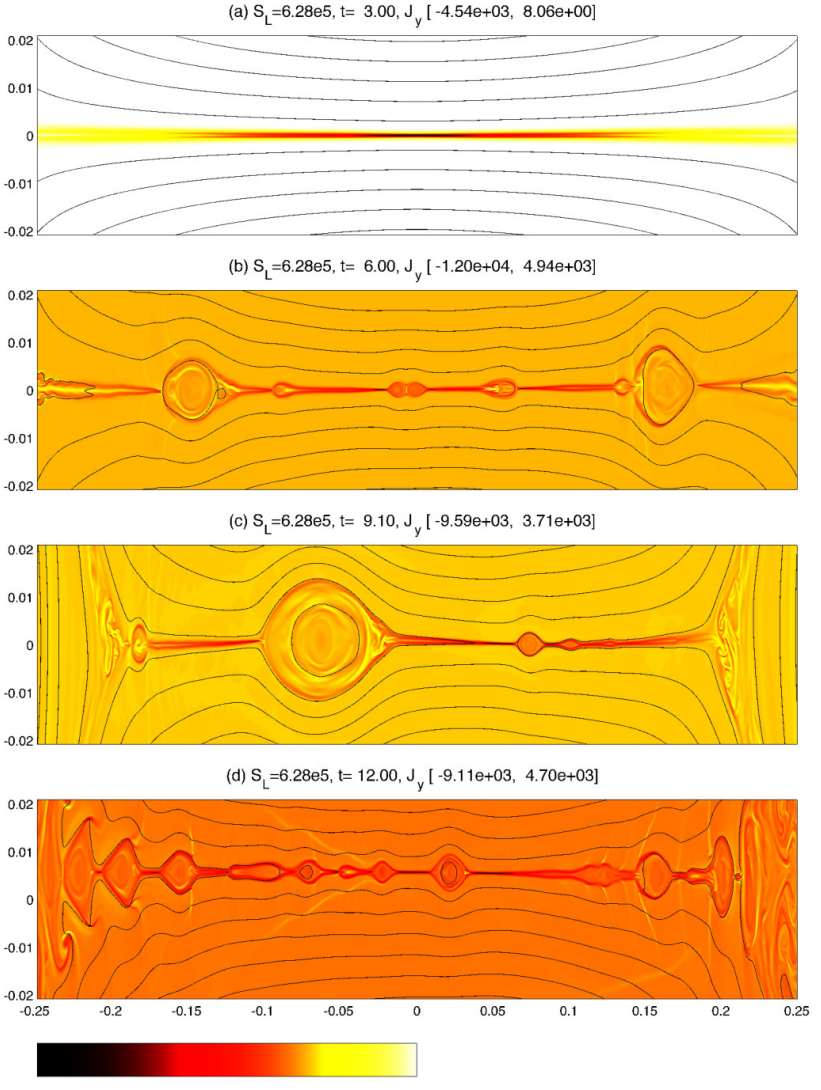

Since then, simulations of plasmoid-dominated reconnection has become an industry.

Given that large-aspect-ratio SP current sheets are violently unstable to the plasmoid instability, it is worth asking whether we should expect them to exist in nature at all. Indeed, Lundquist numbers of typical space and astrophysical plasmas are absurdly large, with $S \sim 10^{13}$ or so in the solar corona implying a plasmoid-instability time scale less than 0.06% of the dynamical time scale. Why would a nice SP current sheet ever be realized under these conditions? See Pucci & Velli (2014) and Uzdensky & Loureiro (2016) for more.[6]

[6]You may also wish to see Alt & Kunz (2019) for reasons why a relatively large-scale, smoothly varying current layer (e.g., a Harris sheet) should not be expected to occur in a weakly collisional, high-β plasma.

REFERENCES

Alt, A. & Kunz, M. W. 2019 Onset of magnetic reconnection in a collisionless, high-beta plasma. *J. Plasma Phys.* **85** (1), 764850101.

Ara, G., Basu, B., Coppi, B., Laval, G., Rosenbluth, M. N. & Waddell, B. V. 1978 Magnetic reconnection and m = 1 oscillations in current carrying plasmas. *Annals of Physics* **112**, 443–476.

Bhattacharjee, A., Huang, Y.-M., Yang, H. & Rogers, B. 2009 Fast reconnection in high-Lundquist-number plasmas due to the plasmoid Instability. *Phys. Plasmas* **16** (11), 112102.

Biskamp, D. 1986 Magnetic reconnection via current sheets. *Physics of Fluids* **29**, 1520–1531.

Biskamp, D. & Schwarz, E. 2001 Localization, the clue to fast magnetic reconnection. *Physics of Plasmas* **8**, 4729–4731.

Daughton, W., Roytershteyn, V., Albright, B. J., Karimabadi, H., Yin, L. & Bowers, K. J. 2009 Transition from collisional to kinetic regimes in large-scale reconnection layers. *Physical Review Letters* **103** (6), 065004.

Erkaev, N. V., Semenov, V. S., Alexeev, I. V. & Biernat, H. K. 2001 Rate of steady-state reconnection in an incompressible plasma. *Physics of Plasmas* **8**, 4800–4809.

Erkaev, N. V., Semenov, V. S. & Jamitzky, F. 2000 Reconnection Rate for the Inhomogeneous Resistivity Petschek Model. *Physical Review Letters* **84**, 1455–1458.

Escande, D. F. & Ottaviani, M. 2004 Simple and rigorous solution for the nonlinear tearing mode. *Physics Letters A* **323**, 278–284.

Furth, H. P., Killeen, J. & Rosenbluth, M. N. 1963 Finite-Resistivity Instabilities of a Sheet Pinch. *Physics of Fluids* **6**, 459–484.

Harris, E. G. 1962 On a plasma sheath separating regions of oppositely directed magnetic field. *Il Nuovo Cimento* **23**, 115–121.

Huang, Y.-M. & Bhattacharjee, A. 2010 Scaling laws of resistive magnetohydrodynamic reconnection in the high-Lundquist-number, plasmoid-unstable regime. *Physics of Plasmas* **17** (6), 062104–062104.

Ji, H., Yamada, M., Hsu, S. & Kulsrud, R. 1998 Experimental Test of the Sweet-Parker Model of Magnetic Reconnection. *Physical Review Letters* **80**, 3256–3259.

Kulsrud, R. M. 2001 Magnetic reconnection: Sweet-Parker versus Petschek. *Earth, Planets, and Space* **53**, 417–422.

Loureiro, N. F., Cowley, S. C., Dorland, W. D., Haines, M. G. & Schekochihin, A. A. 2005 X-Point Collapse and Saturation in the Nonlinear Tearing Mode Reconnection. *Phys. Rev. Lett.* **95** (23), 235003.

Loureiro, N. F., Samtaney, R., Schekochihin, A. A. & Uzdensky, D. A. 2012 Magnetic reconnection and stochastic plasmoid chains in high-Lundquist-number plasmas. *Physics of Plasmas* **19** (4), 042303–042303.

Loureiro, N. F., Schekochihin, A. A. & Cowley, S. C. 2007 Instability of current sheets and formation of plasmoid chains. *Phys. Plasmas* **14** (10), 100703–100703.

Loureiro, N. F., Schekochihin, A. A. & Uzdensky, D. A. 2013 Plasmoid and Kelvin-Helmholtz instabilities in Sweet-Parker current sheets. *Phys. Rev. E* **87** (1), 013102.

Loureiro, N. F. & Uzdensky, D. A. 2016 Magnetic reconnection: from the Sweet-Parker model to stochastic plasmoid chains. *Plasma Phys. Controlled Fusion* **58** (1), 014021.

Malyshkin, L. M., Linde, T. & Kulsrud, R. M. 2005 Magnetic reconnection with anomalous resistivity in two-and-a-half dimensions. I. Quasistationary case. *Physics of Plasmas* **12** (10), 102902–102902.

Militello, F. & Porcelli, F. 2004 Simple analysis of the nonlinear saturation of the tearing mode. *Physics of Plasmas* **11**, L13–L16.

Ni, L., Germaschewski, K., Huang, Y.-M., Sullivan, B. P., Yang, H. & Bhattacharjee, A. 2010 Linear plasmoid instability of thin current sheets with shear flow. *Physics of Plasmas* **17** (5), 052109.

Park, W., Monticello, D. A. & White, R. B. 1984 Reconnection rates of magnetic fields including the effects of viscosity. *Physics of Fluids* **27**, 137–149.

Parker, E. N. 1957 Sweet's Mechanism for Merging Magnetic Fields in Conducting Fluids. *J. Geophys. Res.* **62**, 509–520.

Petschek, H. E. 1964 Magnetic Field Annihilation. *NASA Special Publication* **50**, 425.

Pucci, F. & Velli, M. 2014 Reconnection of Quasi-singular Current Sheets: The "Ideal" Tearing Mode. *Astrophys. J. Lett.* **780**, L19.

Rutherford, P. H. 1973 Nonlinear growth of the tearing mode. *Phys. Fluids* **16**, 1903–1908.

Samtaney, R., Loureiro, N. F., Uzdensky, D. A., Schekochihin, A. A. & Cowley, S. C. 2009 Formation of Plasmoid Chains in Magnetic Reconnection. *Physical Review Letters* **103** (10), 105004.

Sato, T. & Hayashi, T. 1979 Externally driven magnetic reconnection and a powerful magnetic energy converter. *Physics of Fluids* **22**, 1189–1202.

Scholer, M. 1989 Undriven magnetic reconnection in an isolated current sheet. *J. Geophys. Res.* **94**, 8805–8812.

Sweet, P. A. 1958 The Neutral Point Theory of Solar Flares. In *Electromagnetic Phenomena in Cosmical Physics* (ed. B. Lehnert), *IAU Symposium*, vol. 6, p. 123.

Tajima, T. & Shibata, K., ed. 1997 *Plasma astrophysics*.

Ugai, M. 1995 Computer studies on powerful magnetic energy conversion by the spontaneous fast reconnection mechanism. *Physics of Plasmas* **2**, 388–397.

Uzdensky, D. A. & Kulsrud, R. M. 2000 Two-dimensional numerical simulation of the resistive reconnection layer. *Physics of Plasmas* **7**, 4018–4030.

Uzdensky, D. A. & Loureiro, N. F. 2016 Magnetic Reconnection Onset via Disruption of a Forming Current Sheet by the Tearing Instability. *Phys. Rev. Lett.* **116** (10), 105003.

Waelbroeck, F. L. 1993 Onset of the sawtooth crash. *Phys. Rev. Lett.* **70**, 3259–3262.

Yamada, M., Kulsrud, R. & Ji, H. 2010 Magnetic reconnection. *Rev. Mod. Phys.* **82**, 603–664.

Zweibel, E. G. & Yamada, M. 2009 Magnetic Reconnection in Astrophysical and Laboratory Plasmas. *Ann. Rev. Astron. Astrophys.* **47**, 291–332.